

Table of Contents

Advanced Topics in Scattering Theory and Biomedical Engineering
by A. Charalambopoulos, D. I. Fotiadis (Editor)

Overview -

Advanced Topics in Scattering Theory and Biomedical Engineering

Product Details

Pub. Date: August 2010

Publisher: **World Scientific Publishing Company**, Incorporated

Format: Hardcover , 424pp

ISBN-13: 9789814322027

ISBN: 9814322024

Synopsis

The book contains papers on scattering theory and biomedical engineering - two rapidly evolving fields which have a considerable impact on today's research. All the papers are state-of-the-art, have been carefully reviewed before publication and the authors are well-known in the scientific community. In addition, some papers focus more on applied mathematics, which provides a solid ground for development and innovative research in scattering and biomedical engineering.

From the Publisher

Advanced Topics in Scattering Theory and Biomedical Engineering

Table of Contents

Preface

1. Mathematical Methods in Scattering and Biomedical Engineering 1
2. The Double Analytic Structure that allows the Introduction of Vector Ellipsoidal Harmonics G. Dassios 3
3. The Inverse Scattering Problem in Linear Elasticity via a pair of Non-Linear Integral Equations D. Gintides L. Midrinos 12
4. Low- Frequency Modeling of the Interaction of a Magnetic Dipole and Two Metallic Spherical Bodies in a Conductive Medium P. Vafeas D. Lesselier 20
5. Size Effects in the Mechanical Properties of Carbon Nanotubes K.I. Tserpes S. Pantelakis 28
6. Biomedical Engineering 37
7. Photon scattering applications in tissue characterisation and imaging R. Speller 39
8. Low frequency scattering by a soft acoustic sphere embedded into an acoustically lossless half space J.L. Lekatsas V. Kostopoulos 55
9. An Automated Method for Atherosclerotic Plaque Characterization and Quantification using Intravascular Ultrasound Images L.S. Athanasiou D.I. Fotiadis V.D. Tsakanikas K.K. Naka L.K. Michalis 63
10. **The impact of scattering and peak spectrum of I-123 in scintigraphy by I-123 MIBG**, M.E. Lyra N. Lagopati M. Sotiropoulos Ch. Chatzigiannis M. Gavrielli 79
11. Predictive Medicine: CFD Techniques in severe Renal Artery Stenosis to facilitate Therapeutic Decision-Making E.D. Skouras G.C. Bourantas V.C. Loukopoulos E.N. Liatsikos G.C. Nikiforidis 90
12. Point - of - care Monitoring and Diagnostics for Rheumatoid Arthritis and Multiple Sclerosis F.G. Kalatzis T.P. Exarchos N. Gionnakeas P. Rizos D.I. Fotiadis S. Markoula E. Hatzi I. Georgiou 98
13. DNA: The Axioms of Cell Geometry the Differential Geometry of its Function the Affine Geometry of its Structure I.L. Arahovitis 106
14. Prediction of atherosclerotic plaque formation based on LDL transport for a 3D patient specific coronary artery with deformable walls A.I. Sakellarios M.I. Papafaklis C.V. Bourantas L.K. Michalis D.I. Fotiadis 114
15. Setting a Rational Framework for Experimental Design and Analysis of High - Throughput DNA Microarray Experiments and Data G.I. Lambrou A. Chatziioannou E. Sifakis A. Prentza D. Koutsouris E. Koulouki F. Tzortzatos-Stathopoulou 122
16. A clustering-based method for gene expression comparison in embryonic stem cell derived hemangioblasts and adult bone marrow stromal cells L. Maglaras D.I. Fotiadis I. Georgiou 130
17. Morphological Image Denoising and Random - Walks Spot Detection in Microarray Images A. Mastrogianni E. Dermatas A. Bezerianos 143
18. Electromagnetic Scattering and Biomedical Applications 151
19. Removing Non Uniform Illumination Effects in Infrared Images M. Vlachos E. Dermatas 153

THE IMPACT OF SCATTERING AND PEAK SPECTRUM OF I-123 IN SCINTIGRAPHY BY I-123 MIBG

M.E. LYRA, N. LAGOPATI AND M. SOTIROPOULOS

*University of Athens, Dep. of Radiology, Radiation Physics Unit
Athens 11528, Greece
mlyra@med.uoa.gr*

CH. CHATZIGIANNIS AND M. GAVRILELLI

*Medical Imaging Center, Nuclear medicine section
Athens 11525, Greece
mlyra@medimaging.gr*

Metaiodobenzylguanidine (MIBG) scintigraphy is used to image tumors of neuroendocrine origin and study disorders of sympathetic innervation of the myocardium. Scintigraphic imaging methods offer the possibility of qualitative and quantitative assessment of tracer concentration. Accurate correction for the physical degrading factors (attenuation, scatter, partial volume effects) is demanded. An analytical study of the I-123 energy spectrum, scattering and attenuation contribution to the resulting image of an I-123 MIBG scintigraphy, has been undergone, so as to improve the data that could be collected by I-123-MIBG use. In this work, quantitative data were gathered at various source depths, volumes and crystal to phantom distances to determine the effect of these variables on source activity data. The final image is being extracted from the combination of three different images, each and every one being acquired by a different energy window. The middle one has been obtained from the main I-123 photopeak and the others, from the left and right peaks respectively. The problem of Compton scattering as the dominant photon interaction phenomenon and its impact on both the quality of clinical images and the accuracy of quantitative analysis is taken into consideration for a scatter modeling in non-uniform media.

1. Introduction

The main objective of the X-ray imaging is the optimization of the diagnostic procedure for a better image quality/patient dose ratio. The most important factor affecting the image quality is the scattered component of the radiation resulting from the interactions of photons within the object being radiographed. It is therefore of great importance to investigate both theoretical and experimental scatter data such as scatter fractions, spectral and angular distributions of the scattered radiation under diagnostic imaging conditions.

The contribution of the scattered radiation to the image quality has been estimated by many investigators (Barnea and Dick, 1986 [1]; Dick et al., 1986; Chan and Doi, 1983) using the scatter fraction F defined as:

$$F = \frac{N_T - N_U}{N_T} \quad (1)$$

where N_T is the total number of (scattered and unscattered) photons at the detector in place and N_U is the unscattered component of N_T . Theoretical investigation of the properties of scattered radiation have been attempted.

As Compton scattering plays a key role, we will recall some of its properties. The Compton Effect discovered in 1923 [2] had served to confirm the particle (photon) nature of radiation, as proposed by A. Einstein. Thus, energetic radiation under the form of X- or gamma-rays behaves like particles and scatter with electrically charged particles in matter [3], [4]. In biomedical domains, X- or gamma-photons scatter electrons in the biological media they traverse. More specifically, in classical (Thomson and Rayleigh) scattering, the scattered radiation has the same wavelength as the incident radiation and no energy is transferred [5]. In a Compton collision or an incoherent scattering event, energy transferred to an electron, which recoils from the collision. Since energy and momentum are conserved, we may analyze the process in detail using the fig.1.

Let $h\nu$ and p represent the energy and the momentum of the incident photon, $h\nu'$ and p' corresponding parameters for the scattered photon. The momentum, p , of a photon of energy $h\nu$ is simply $h\nu/c$. Let the electron recede from the collision with energy E , momentum q , and velocity v . [6], [7]. Since the electron may have velocity comparable with c it is necessary to use the relativistic expressions for its kinetic energy and momentum thus:

$$h\nu - h\nu' = E = m_0 c^2 \left\{ \frac{1}{\sqrt{1 - v^2/c^2}} - 1 \right\} \quad (2)$$

Since momentum is also conserved, the sum of the vectors p' and q must equal p ; this means p , q , and p' form the sides of a triangle, so that

$$q^2 = p^2 + (p')^2 - 2pp' \cos \theta \quad (3)$$

or we can write down expressions for the conservation of momentum in the forward direction

$$\frac{h\nu}{c} = \frac{h\nu'}{c} \cos \theta + \frac{m_0 v}{\sqrt{1 - v^2/c^2}} \times \cos \varphi \quad (4)$$

and in the direction at right angles to give

$$\frac{h\nu'}{c} \sin \theta = \frac{m_0 v}{\sqrt{1 - v^2/c^2}} \times \sin \varphi \quad (5)$$

By eliminating v and φ , the reader may show that:

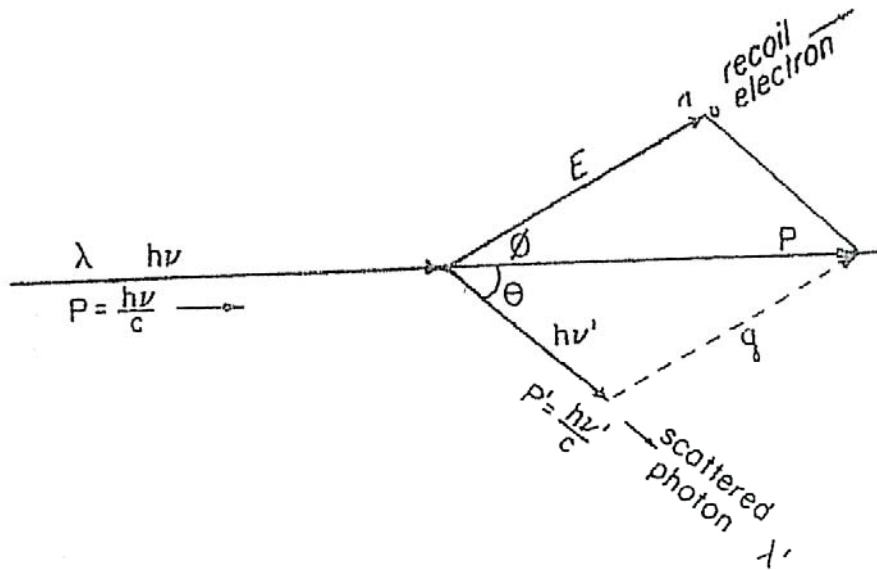
$$E = h\nu \cdot \frac{\alpha (1 - \cos \theta)}{1 + \alpha (1 - \cos \theta)} \quad (6)$$

$$h\nu' = h\nu \cdot \frac{1}{1 + \alpha (1 - \cos \theta)} \quad (7)$$

where

$$\alpha = \frac{h\nu}{m_0 c^2} = \frac{h\nu (MeV)}{0,511} \quad (8)$$

The parameter α is the ratio of the energy of the photon to the rest energy of the electron ($m_0 c^2$). If the energy of the photon is impressed in MeV, then $m_0 c^2 = 0,511$ MeV [7], [8]. By adding the electron energy, E , to the energy of the scattered photon, $h\nu'$ one obtains the incident energy $h\nu$ in agreement with the first equation.



In this work, a preliminary study in Metaiodobenzylguanidine (MIBG) scintigraphy which is used to image tumors of neuroendocrine origin [9] and study disorders of sympathetic innervation of the myocardium has undergone. Scintigraphic imaging methods, generally offer the possibility of qualitative and quantitative assessment of tracer concentration. Then, accurate correction for the physical degrading factors (attenuation, scatter, partial volume effects) is demanded. An analytical study of the I-123 energy spectrum, scattering and attenuation contribution to the resulting image of an I-123-MIBG scintigraphy, has been tried to increase and improve the data that could be collected by I-123 -MIBG use.

The endmost plan is to maximize sensitivity for a given crystal geometry, by choosing regions of interest at x -ray gamma and coincidence peaks. Measurements of source activity were found to be independent of the Source Volume [10]. Coincidence counting of measuring I-123 is independent of the counting geometry, the volume and the depth of the source. Corrections for scattering photons improve image quality. Several sources of inaccuracy and inconsistency as radionuclide purity have been shown to affect the quality of imaging, the estimation of uptake measurements and the absorbed dose of the patient. Depths, position, volume of the organ are other factors that increase the scattering effect.

More than one energy range, in the spectrum, scattering, x-ray, gamma-peak, impurities' peaks and coincidence peak, were selected to be studied. Aim was to increase statistics of the data, improve the image of the organ, without increase of the absorbed dose in the patient.

2. Materials and methods

Phantom studies were performed to determine the feasibility of exploiting the scattering, x-ray and coincidence peaks as well as the low peaks of I-123 impurities. Quantitative data were gathered at various source depths, volumes and crystal to phantom distances to determine the effect of these variables on source activity data.

2.1 Triple Energy Window method [TEW]

In this method the final image is being extracted from the combination of three different images, each and every one being acquired by a different energy window. Planar images were acquired by GE tomographic gamma - camera.

The middle one has been obtained from the main I-123 photopeak and the others are from the left and right peaks respectively. Many different window widths have been proposed. The most useful configuration is a 20% central window with a 10 keV upper and lower sub windows, as proposed by ref. [11].

When the counts on lower, central and upper window are defined as CL , CC , CU , and the corresponding widths as WL , WC and WU respectively then the corrected image can be written as:

$$C_{corrected} = CC - \left(\frac{CL}{WL} + \frac{CU}{WU} \right) \cdot \frac{WC}{2} \quad (9)$$

As it is shown from the former formula, the counts of a trapezoid inside the photopeak are being estimated. Furthermore the counts of this trapezoid can estimate the Compton contamination of the photopeak (figure 2).

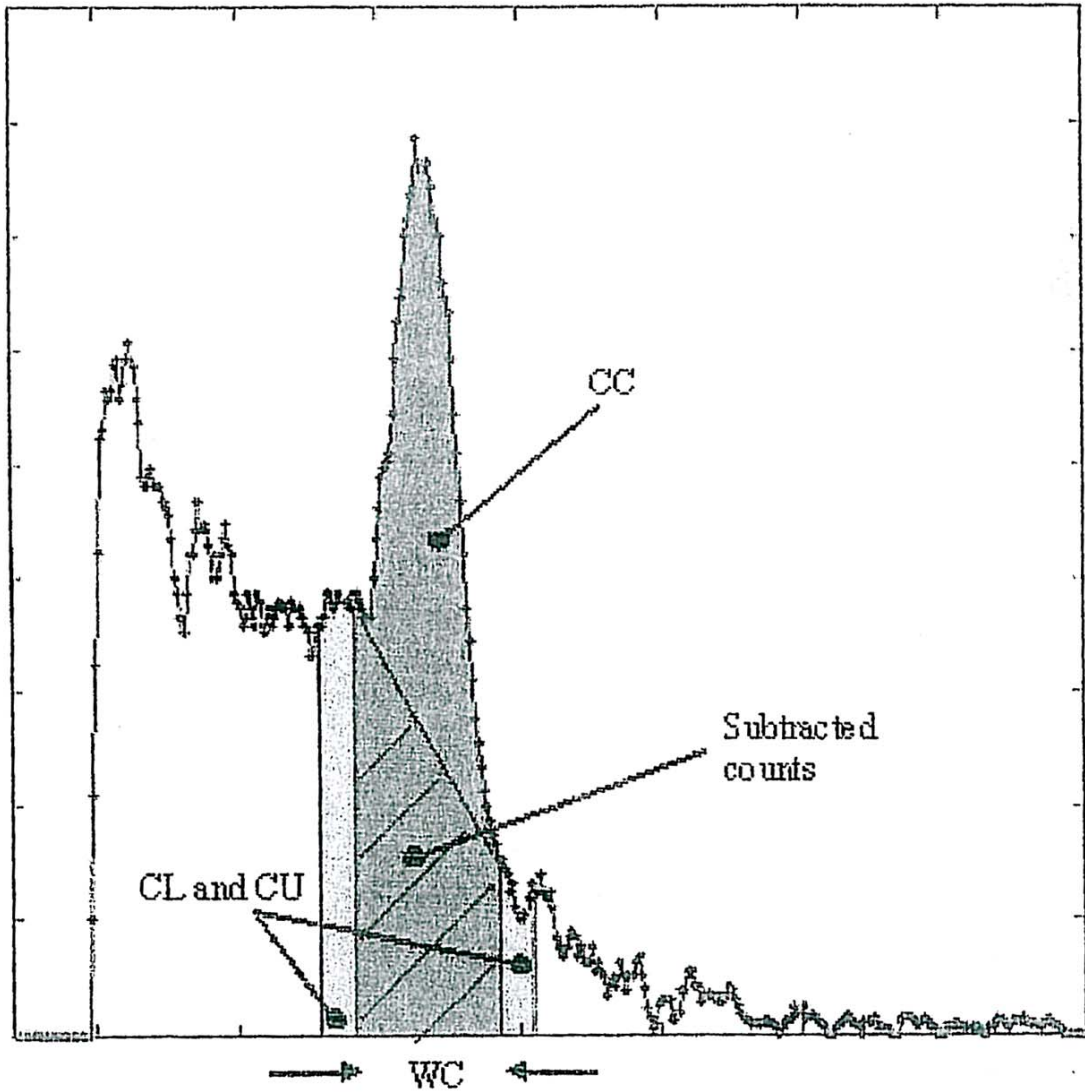


Figure 2. This is a schematic representation of the 1123 triple energy window [TEW] method.

2.2 Spectra Simulation

A simple Monte Carlo code was developed to simulate Compton scattering. The energy spectra can be assumed that consists of the main peak photons and the summation of the sequentially scattered photons [13], [14].

$$F(E_0, E) = W_0 \cdot P(E_0, E) + \sum W_i F_i(E_0, E) \quad (10)$$

where i determines the Compton scattering order and $P(E_0, E)$ is the energy spread function of the gamma camera at energy E_0 ,

which, can approximated be expressed by the Gaussian form of

$$P (E_0 , E) = \exp \left[\frac{-4 \ln 2 (E - E_0)^2}{R^2} \right] \quad (11)$$

Where, R is the energy resolution of the γ -camera.

Compton scattering was simulated by Klein-Nishina cross section formula [6], [14] and an analytical form for the *incoherent scattering factor* [15], [16], which is widely used in many Monte-Carlo codes. No photoelectric absorption was simulated, due to the high probability of the Compton effect.

In this work, the scattering part of the spectra has been simulated by the first six scatter spectra. The spectrum consists of 512 discrete energies, which makes satisfying a simulation of 100000 initial events.

Furthermore the best fit of this ideal spectrum was estimated, by optimizing of the W_i parameters of the equation (10) making possible the estimation of the scattered photons in the photopeak.

3. Results

3.1 Image analysis

Image processing at the scintigraphic images of a 5 years-old girl, were undergone using the TEW method. Contrasts of background and kidney as well as heart to kidney ratio (HKR) were calculated (figure 3 and 4).

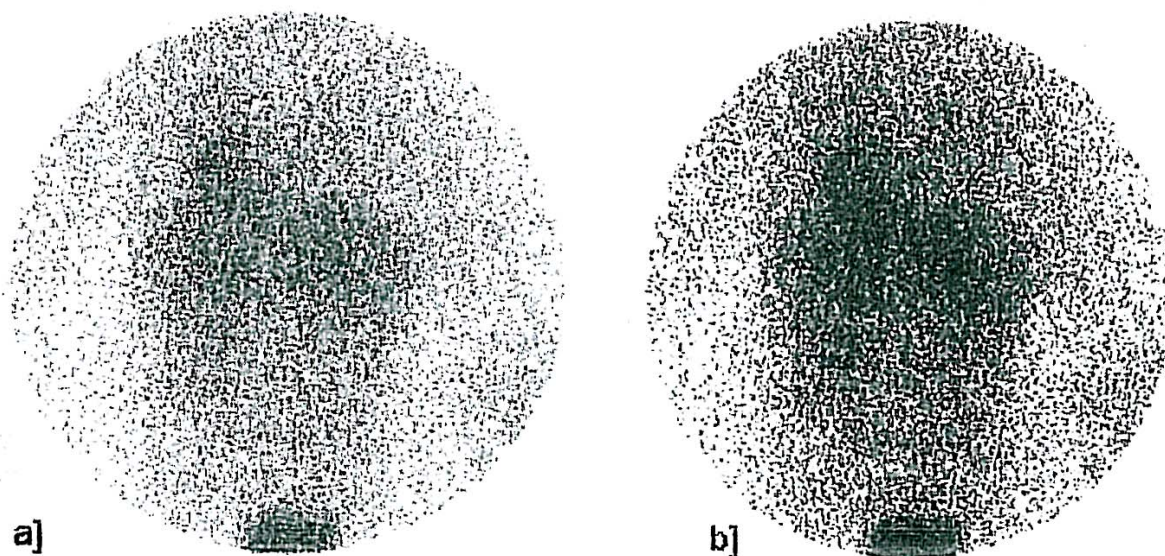


Figure3. Images of I-123-MIBG acquisitions of a patient a) before and b) after TEW method application. Heart to kidney ratio (HKR) calculation.

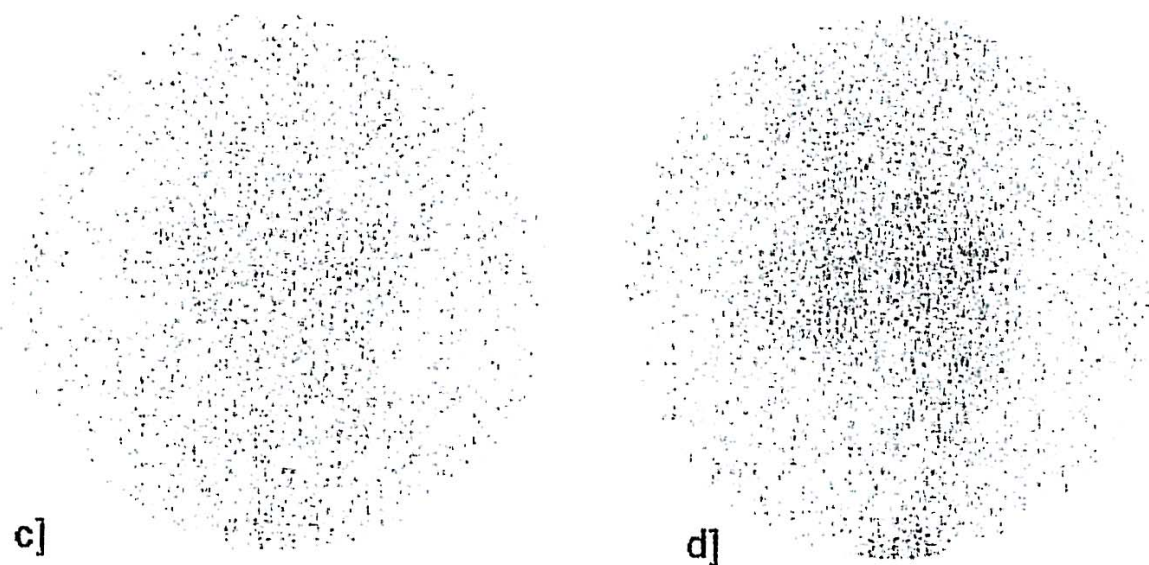


Figure4. Images of low c) and upper d) energy window acquisitions of a patient injected by I-123-MIBG

Contrast, defined as $100 \% * (Bg-ROI)/Bg$, is improved from 42% to 72% and HKR from 3.56 to 4.48.

3.2 *Quantitative analysis*

The ratio of the total counts of the spectrum to the scattered counts (TS) in the width of the used photopeak window has been calculated in order to quantify the Compton counts in the photopeak and the total effect of it, as

well as. Background has been subtracted in both methods. No events from the 689 keV (1.4%) peak have been simulated, as mentioned above. TEW method estimates TS of 2.15 while the simulated data estimate TS of 7.69. Figure5 shows the calculated spectrum. (measured, simulated, photopeak, total scatter and scattering components)

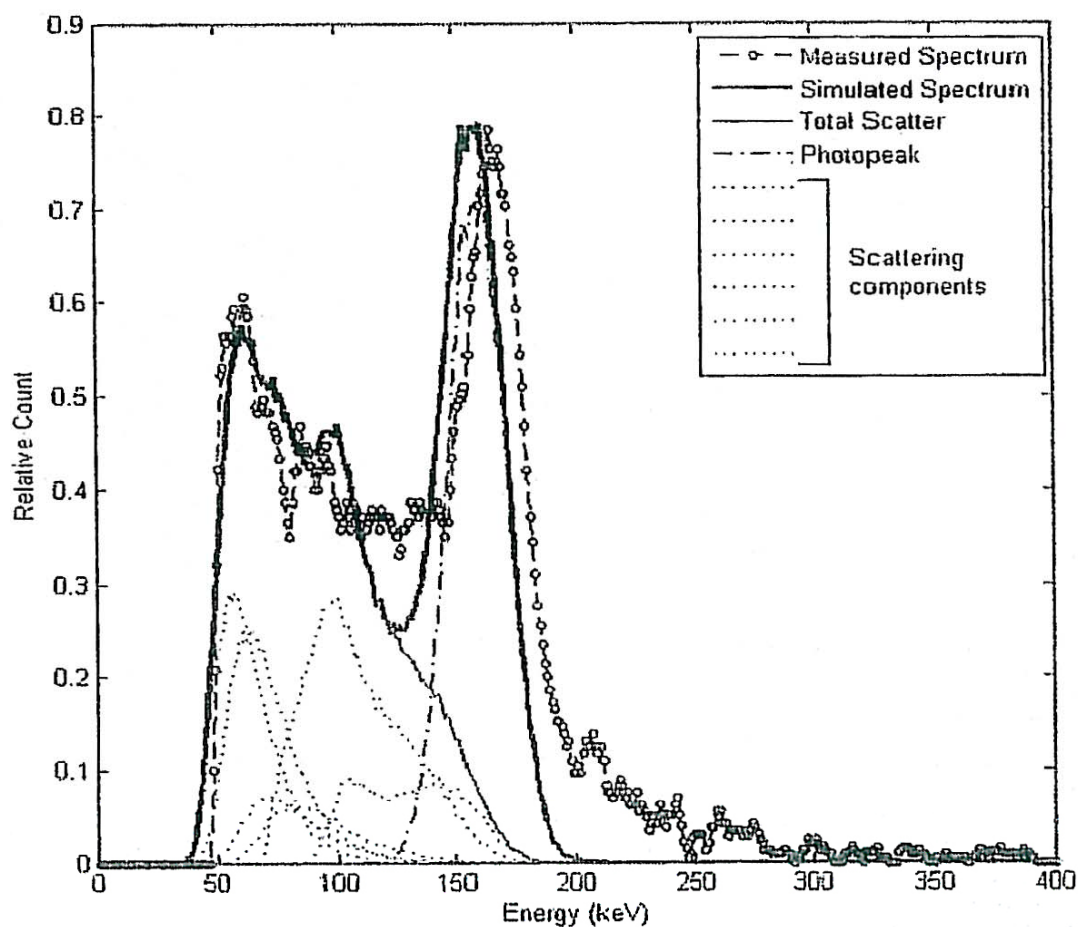


Figure5. The spectrum as has been calculated (measured and simulated)

4. Discussion

As several sources of inaccuracy and inconsistency as radionuclide purity have been shown to affect the quality of imaging, the estimation of uptake measurements and the absorbed dose of the patient, it is of crucial importance, for us to be able to quantify them, in order to eliminate the negative effect at the resulting image.

Accurate correction for the physical degrading factors (attenuation, scatter, partial volume effects) is demanded [17]. Depths, position, volume of the organ are other factors that increase the scattering effect. Thus, corrections for scattering photons improve image quality and are supposed to be obligatory.

By increasing statistics of the data, we could improve the image of the organ, without increase of the absorbed dose in the patient, which is the ideal outcome.

This was an analytical study of the I-123 energy spectrum, scattering and attenuation contribution to the resulting image of an I-123 MIBG scintigraphy, as an attempt to increase and improve the data that could be collected by I-123-MIBG use.

5. Conclusion

We obtained preliminary evidence that the quality of the image is, by far, better and more accurate, when we choose the specific energy windows, with the triple energy window method, which was analytically described in this work. The further analysis, which is going to give the final touch in the final image, is under investigation.

References

1. G. Barnea, and C.E. Dick, *Med. Phys.* **13**, 490, (1986).
2. A. H. Compton, *Phys. Rev*, vol 21, **5**, 483, (1923).
3. G. Beyklin, vol 37, **5**, 579, (1984).
4. S. R. Deans, *J. Math. Phys*, vol. 19, **11**, 2346, (1978).
5. H. H. Barrett, *Progress in Optics*, E. Wolf, Ed., **21**, 219, (1984).
6. H.E. Johns, and J.R.Cunningham, C6, 173
7. H.E. Johns, and J.R.Cunningham C7, 235
8. S. Helgason, *The randon transform*, pubs Birkhauser, Boston 158, (1999).
9. Lyra M, Phinou P, Papanikolos G et al, *WJNM*,vol.4, S1,33,(2005)
10. T. T. Truong, M. K. Nguyen, and H. Zaidi, *International J Biomed Imag*, **10**, 1155, (2007).
11. K. Nakajima, K. Matsubara et al, *J. Nucl. Card.* **14**, 843 (2007).
12. E. Chen and C. Lam, *Comput. Biol. Med.* **24**, 229 (1994).
13. J.M. Boone, and J.A. Seibert, *Med. Phys.* **15**, 713, (1988a).
14. J. Baro, M. Roteta, J. Fernandez-Varea and F. Salvat, *Radiat. Phys.Chem.* **44**, 531 (1994).